ACADEMIC PRESS

Available online at www.sciencedirect.com

SCIENCE DIRECT®

Journal of Sound and Vibration 268 (2003) 657–678

JOURNAL OF SOUND AND VIBRATION

www.elsevier.com/locate/jsvi

Non-linear parameter estimation with Volterra series using the method of recursive iteration through harmonic probing

Animesh Chatterjee[a], Nalinaksh S. Vyas[b,*]

[a] *Department of Mechanical Engineering, Visvesvaraya National Institute of Technology, Nagpur 440011, India*
[b] *Department of Mechanical Engineering, Indian Institute of Technology, Kanpur 208016, India*

Received 20 May 2002; accepted 21 November 2002

Abstract

Volterra series provides a platform for non-linear response representation and definition of higher order frequency response functions (FRFs). It has been extensively used in non-parametric system identification through measurement of first and higher order FRFs. A parametric system identification approach has been adopted in the present study. The series response structure is explored for parameter estimation of polynomial form non-linearity. First and higher order frequency response functions are extracted from the measured response harmonic amplitudes through recursive iteration. Relationships between higher order FRFs and first order FRF are then employed to estimate the non-linear parameters. Excitation levels are selected for minimum series approximation error and the number of terms in the series is controlled according to convergence requirement. The problem of low signal strength of higher harmonics is investigated and a measurability criterion is proposed for selection of excitation level and range of excitation frequency. The procedure is illustrated through numerical simulation for a Duffing oscillator. Robustness of the estimation procedure in the presence of measurement noise is also investigated.

1. Introduction

The functional form representation of input–output relationship through Volterra series provides a structured mathematical platform for the study of non-linear systems. It employs multi-dimensional kernels, which upon convolution with the applied excitation forces, express system response in the form of a power series. Frequency domain transforms of these multi-dimensional kernels provide higher order kernel transforms or frequency response functions

*Corresponding author. Fax: +91-512-590007.
E-mail addresses: animeshch@rediffmail.com (A. Chatterjee), vyas@iitk.ac.in (N.S. Vyas).

0022-460X/03/$ - see front matter © 2002 Elsevier Science Ltd. All rights reserved.
doi:10.1016/S0022-460X(02)01537-7

(FRFs). For harmonic excitations, the response can be conveniently expressed in terms of the first and higher order FRFs.

Non-parametric system identification through measurement of the higher order FRFs has been an area of extensive research. Boyd et al. [1] developed a second order kernel transform measurement procedure using multi-tone harmonic probing. Chua and Liao [2] extended the procedure for third and higher order kernel transforms. Gifford and Tomlinson [3] developed a multi-degree-of-freedom curve-fitting procedure for estimating the higher order FRFs. Storer and Tomlinson [4] and Gifford [5] have discussed procedures for experimental measurement of higher order kernel transforms with truncated response series. A survey on non-linear dynamic system structure identification can be found in the recent paper of Haber and Unbehauen [6].

Volterra series, being a power series, suffers from the inherent problem of limited convergence. Tomlinson and Manson [7] studied the convergence of first order FRF of a Duffing oscillator under harmonic excitation and presented a simple formula for determining the upper limit of excitation level for series convergence at the natural frequency of the system. Chatterjee and Vyas [8] defined a critical value of the non-dimensional non-linear parameter for response harmonic series convergence and observed that the limiting value of the parameter is a function of excitation frequency and number of terms, k, in the response series approximation. Research works available in the area of parametric system identification through Volterra series, however, are very few. For a polynomial form of non-linearity, higher order Volterra kernel transforms can be shown to be related to the first order kernel transforms through the set of non-linear parameters. This relationship provides a mathematical platform for estimating the parameters from the measured kernel transforms. Lee [9] has extracted the response components of first harmonic amplitude through response component separation technique and measured the first and higher order kernel transforms. Parameters were then estimated using the relationship between higher and first order transforms.

The present method suggests an approach, where response amplitudes of first and higher order harmonics are measured and the non-linear parameters along with the first order kernel transforms are estimated through the recursive iteration technique. The iteration corrects for the contribution of higher order terms in the response harmonic series up to the convergence threshold and provides a refined estimate of the first and higher order kernel transforms. Non-linear parameters are estimated using the higher order kernel synthesis relationship. Excitation amplitudes over a wide range of frequencies are decided from the response series convergence criterion [8]. Criteria for selecting excitation frequency for the maximum signal strength of higher harmonics are discussed. Numerical simulation is carried out for a typical Duffing oscillator and robustness of the estimation procedure in the presence of random noise is also investigated.

2. Volterra series representation of response harmonic amplitudes

Volterra series response representation for a general physical system with $f(t)$ as input excitation and $x(t)$ as output response is given by

$$x(t) = x_1(t) + x_2(t) + x_3(t) + \cdots + x_n(t) + \cdots, \tag{1}$$

with

$$x_n(t) = \int_{-\infty}^{\infty} \cdots \int_{-\infty}^{\infty} h_n(\tau_1, \ldots, \tau_n) f(t-\tau_1) \cdots f(t-\tau_n)\, \mathrm{d}\tau_1 \cdots \mathrm{d}\tau_n. \tag{2}$$

$h_n(\tau_1, \ldots, \tau_n)$ is the nth order Volterra kernel and its Fourier transform provides the nth order FRFs or Volterra kernel transforms as

$$H_n(\omega_1, \ldots, \omega_n) = \int_{-\infty}^{\infty} \cdots \int_{-\infty}^{\infty} h_n(\tau_1, \ldots, \tau_n) \prod_{i=1}^{n} \mathrm{e}^{-\mathrm{j}\omega_i\tau_i}\, \mathrm{d}\tau_1 \cdots \mathrm{d}\tau_n. \tag{3}$$

For a single-tone harmonic excitation

$$f(t) = A\cos\omega t = \frac{A}{2}\mathrm{e}^{\mathrm{j}\omega t} + \frac{A}{2}\mathrm{e}^{-\mathrm{j}\omega t}, \tag{4}$$

the expression for the nth order response component, following Eq. (2), can be obtained as

$$x_n(t) = \left(\frac{A}{2}\right)^n \sum_{p+q=n} {}^nC_q H_n^{p,q}(\omega)\mathrm{e}^{\mathrm{j}\omega_{p,q}t}, \tag{5}$$

where the following brief notations have been used:

$$H_n^{p,q}(\omega) = H_n(\underbrace{\omega, \ldots, \omega}_{p\text{times}}, \underbrace{-\omega, \ldots, -\omega}_{q\text{times}}), \quad \omega_{p,q} = (p-q)\omega.$$

The total response of the system then becomes

$$x(t) = \sum_{n=1}^{\infty} \left(\frac{A}{2}\right)^n \sum_{p+q=n} {}^nC_q H_n^{p,q}(\omega)\mathrm{e}^{\mathrm{j}\omega_{p,q}t}. \tag{6}$$

Combinations of different p and q results in various response harmonics at frequencies $\omega_{p,q} = \omega$, 2ω, 3ω, etc. and the response series given in Eq. (6) can be written in terms of its harmonics as

$$x(t) = X_0 + |X(\omega)|\cos(\omega t + \phi_1) + |X(2\omega)|\cos(2\omega t + \phi_2) + |X(3\omega)|\cos(3\omega t + \phi_3) + \cdots, \tag{7}$$

where the response harmonic amplitudes, $X(n\omega)$, are obtained by collecting all the terms associated with the exponential $\mathrm{e}^{\mathrm{j}\omega_{p,q}t}$ in Eq. (6) for $\omega_{p,q} = (p-q)\omega = n\omega$ and are given by

$$X_0 = \sum_{n=1}^{\infty} \left(\frac{A}{2}\right)^{2n} {}^{2n}C_n H_{2n}^{n,n}(\omega),$$

$$X(n\omega) = \sum_{i=1}^{\infty} \sigma_i(n\omega) \quad \text{and} \quad \phi_n = \angle X(n\omega), \tag{8}$$

with

$$\sigma_i(n\omega) = 2\left(\frac{A}{2}\right)^{n+2i-2} {}^{n+2i-2}C_{i-1} H_{n+2i-2}^{n+i-1,i-1}(\omega). \tag{9}$$

For a system with polynomial form of non-linearity given by

$$m\ddot{x}(t) + c\dot{x}(t) + k_1 x(t) + k_2 x^2(t) + k_3 x^3(t) = f(t), \tag{10}$$

the higher order kernel transforms are related to the lower order kernel transforms through non-linear parameters [8] as

$$H_n^{p,q}(\omega) = -\frac{H_1(\omega_{p,q})}{{}^nC_q}\left[k_2 \sum_{\substack{p_i+q_i=n_i \\ n_1+n_2=n}} \left\{{}^{n_1}C_{q_1} H_{n_1}^{p_1,q_1}(\omega)\right\}\left\{{}^{n_2}C_{q_2} H_{n_2}^{p_2,q_2}(\omega)\right\}\right.$$

$$\left. + k_3 \sum_{\substack{p_i+q_i=n_i \\ n_1+n_2+n_3=n}} \left\{{}^{n_1}C_{q_1} H_{n_1}^{p_1,q_1}(\omega)\right\}\left\{{}^{n_2}C_{q_2} H_{n_2}^{p_2,q_2}(\omega)\right\}\left\{{}^{n_3}C_{q_3} H_{n_3}^{p_3,q_3}(\omega)\right\}\right]$$

$$\text{for } n > 1. \tag{11}$$

A higher order kernel transform, thus can be synthesized using Eq. (11), from the values of first order transforms and the non-linear parameters.

3. Recursive iteration

A single-degree-of-freedom model with polynomial non-linearity in stiffness force, as given in Eq. (10), is considered here for estimation of the non-linear parameters k_2, k_3 and the linear parameters m, c and k_1. The response harmonic series (8) is truncated after a finite number of terms, k, and re-arranged for the first three response harmonics to give

$$H_1(\omega) \approx \frac{1}{A}\left[X(\omega) - \sum_{i=2}^{k} \sigma_i(\omega)\right], \tag{12a}$$

$$H_2(\omega,\omega) \approx \frac{2}{A^2}\left[X(2\omega) - \sum_{i=2}^{k} \sigma_i(2\omega)\right], \tag{12b}$$

$$H_3(\omega,\omega,\omega,) \approx \frac{4}{A^3}\left[X(3\omega) - \sum_{i=2}^{k} \sigma_i(3\omega)\right]. \tag{12c}$$

The higher order kernel transforms, $H_2(\omega,\omega)$ and $H_3(\omega,\omega,\omega)$ are related to the first order kernel transform and non-linear parameters (using Eq. (11)) as

$$H_2(\omega,\omega) = -k_2 H_1^2(\omega) H_1(2\omega), \tag{13a}$$

$$H_3(\omega,\omega,\omega) = H_1^3(\omega) H_1(3\omega)\left[2k_2^2 H_1(2\omega) - k_3\right]. \tag{13b}$$

The above Eqs. (13a) and (13b) provide the basis for determination of the non-linear parameters k_2 and k_3 from the measured first, second and third order kernel transforms $H_1(\omega)$, $H_2(\omega,\omega)$ and $H_3(\omega,\omega,\omega)$. The truncated series $\sum_{i=2}^{k} \sigma_i(n\omega)$ in Eq. (12) is computed at every step of iteration with the estimated values of first order kernel transforms, $H_1(\omega)$, and non-linear parameters, k_2 and k_3, obtained from the previous step. Employing Eqs. (12) and (13), linear and non-linear parameters are re-estimated and the iteration is continued till the estimates converge within a

specified limit. For a typical Duffing oscillator, the estimation algorithm can be structured through the following steps.

Step I: The system is excited at frequencies, ω_i, with ω_i varying over a frequency range encompassing the natural frequency, ω_n, of the system. Harmonic amplitude, $X(\omega_i)$, is filtered from the overall response, $x(t)$, which gives the preliminary estimate of first order kernel transform as

$$H_1(\omega_i) = X(\omega_i)/A_i, \quad i = 1, \ldots, N, \tag{14}$$

where A_i is the excitation level selected for frequency ω_i. A curve-fitting procedure [10] is employed to obtain the best-fit FRF curve and preliminary estimation of linear parameters is made.

Step II: The system is excited at a selective range of frequencies, ω_j, $j = 1, 2, \ldots, N$, where the third response harmonic, $X(3\omega_j)$, is distinct and measurable. Employing Eq. (13b), the preliminary estimate of non-linear parameter, k_3, is obtained through regression between the estimated third order kernel transform and its synthesized kernel factor, $\Gamma_3(\omega_j)$, using the following relationship:

$$H_3(\omega_j, \omega_j, \omega_j) = k_3 \Gamma_3(\omega_j), \tag{15}$$

where

$$\Gamma_3(\omega_j) = -H_1^3(\omega_j) H_1(3\omega_j). \tag{16}$$

Step III: The series $\sum_{i=2}^{k} \sigma_i(\omega)$ is computed with the $H_1(\omega)$ values taken from the best-fit curve estimated in Step I and the non-linear parameter, k_3, estimated in *Step* II and substituted in Eq. (12a) to obtain new estimates of linear parameters.

Step IV: The series $\sum_{i=2}^{k} \sigma_i(3\omega)$ is computed and substituted in Eq. (12c) to refine the estimate of the non-linear parameter k_3.

Iteration is continued till the estimate of non-linear parameter, k_3, converges within a specified limit. The algorithm is general in nature and can be readily extended to a system with square or combined square and cubic form of non-linearity. However, for accurate and convergent parameter estimation, the following issues need to be addressed:

(i) selection of appropriate excitation levels, A_i, in Eq. (14) for error minimization in first response harmonic measurement,
(ii) selection of limiting number of terms, k, in Eqs. (12a) and (12c) for convergent Volterra series application,
(iii) selection of appropriate excitation frequency and amplitude for good measurability of higher response harmonics.

4. Convergence and error limits

A detailed convergence and error analysis has been done by the authors in an earlier work [8] in terms of non-dimensional non-linear parameter $\lambda_3 = k_3 A^2/k_1^3$ and non-dimensional frequency $r = \omega/\omega_n$. For a Duffing oscillator, the equation of motion can be written in non-dimensional form as

$$\eta''(\tau) + 2\varsigma\eta'(\tau) + \eta(\tau) + \lambda_3 \eta^3(\tau) = \cos r\tau, \tag{17}$$

where

$$\tau = \omega_n t, \quad \omega_n = \sqrt{k_1/m}, \quad \varsigma = c/2m\omega_n, \quad \eta = xk_1/A.$$

($'$) denotes differentiation with respect to τ. The non-dimensional response $\eta(\tau)$ is filtered to obtain various harmonic amplitudes $Z(nr)$ given by

$$Z(nr) = \sum_{i=1}^{\infty} \sigma_i(nr), \tag{18}$$

where the individual series term, $\sigma_i(nr)$, similar to Eq. (9), becomes

$$\sigma_i(nr) = 2\left(\frac{1}{2}\right)^{n+2i-2} {}_{n+2i-2}C_{i-1} H_{n+2i-2}^{n+i-1,i-1}(r). \tag{19}$$

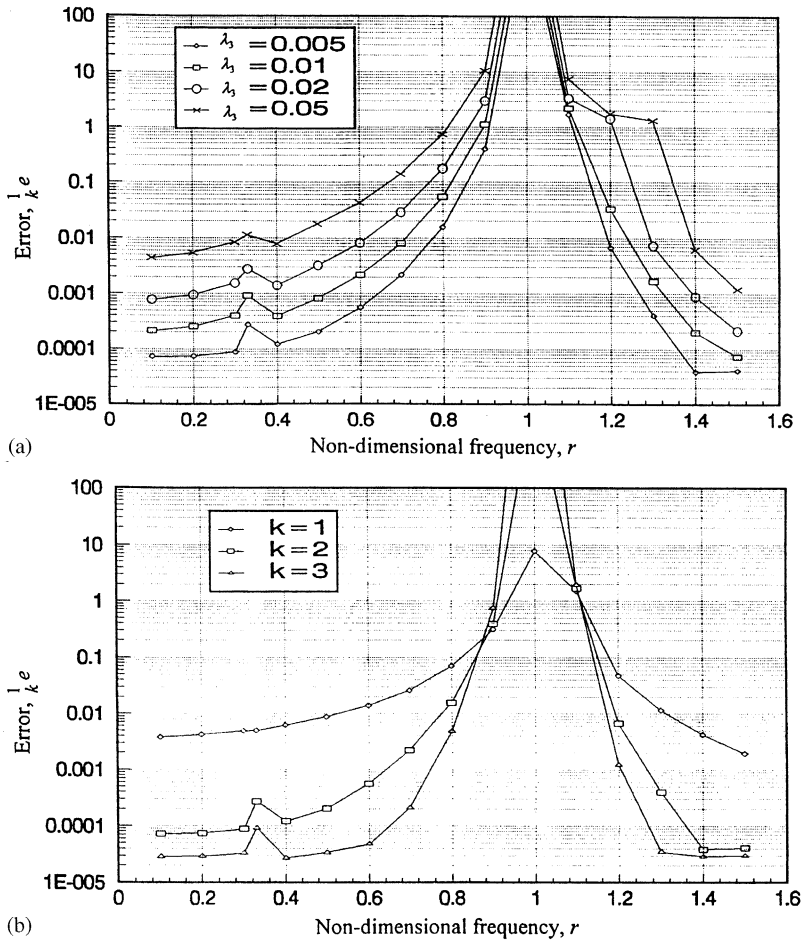

Fig. 1. Variation of approximation error in first response harmonic: (a) [$k = 2$], (b) $\lambda_3 = 0.005$.

A k-term approximation of the response harmonic amplitude can be defined as

$$ {}_kZ(nr) = \sum_{i=1}^{k} \sigma_i(nr). \tag{20} $$

The relative error between the above approximation and the exact value of the response amplitude of the nth harmonic is

$$ {}^n_k e = \left| [Z(nr) - {}_k Z(nr)]/Z(nr) \right|. \tag{21} $$

The critical non-dimensional parameter, ${}^n_k\lambda_{crit}$, can be defined, for a k-term approximation of the nth harmonic, as the limiting value of λ_3, for which

$$ \left| \frac{\sigma_k(nr)}{\sigma_{k-1}(nr)} \right| = 1.0. \tag{22} $$

This ratio test is employed for investigating the convergence of the response harmonic series in Eq. (12) and the series is computed with an optimum number of series terms, k, which satisfies the

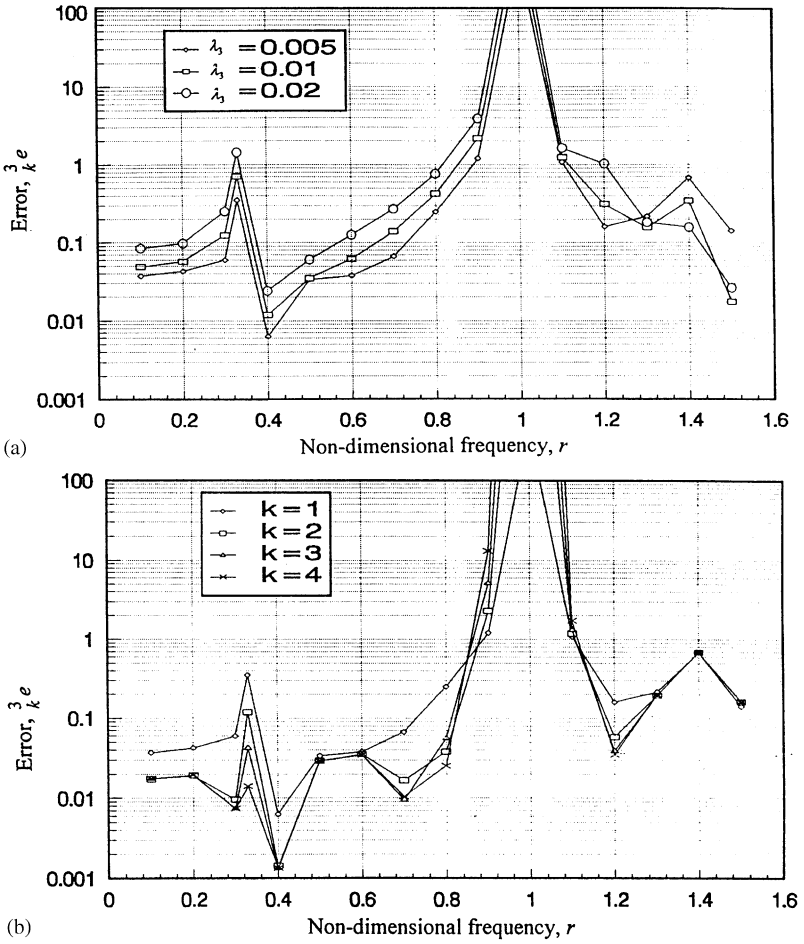

Fig. 2. Variation of approximation error in third response harmonic: (a) [$k = 1$], (b) $\lambda_3 = 0.01$.

ratio test. For a given k-term series approximation, the error, ${}_k^n e$, is a function of the excitation frequency and amplitude. Fig. 1(a) shows the error variation, for a two-term approximation in the first harmonic amplitude $Z(r)$, over a frequency range, for constant excitation levels (i.e., for constant λ_3 values). It can be seen that the error increases with the increase in excitation amplitude and becomes very large near the natural frequency (i.e., $r = \omega/\omega_n = 1$). Fig. 1(b) shows error for different number of terms in the series for a given excitation level, $\lambda_3 = 0.005$. It is seen that the high error near natural frequency increases further with more terms in the series. Similar error characteristics for third harmonic amplitude $Z(3r)$ are shown in Figs. 2(a) and (b).

Reduction of the error in the vicinity of the natural frequency of the system would require a reduction in the amplitude of the excitation force. Variation of the excitation amplitude over the frequency range in such a manner that a constant error level is maintained throughout the frequency range can be suggested for consistency in results. Figs. 3(a) and (b), show the required variation of excitation level in terms of the non-dimensional non-linear parameter λ_3 over the

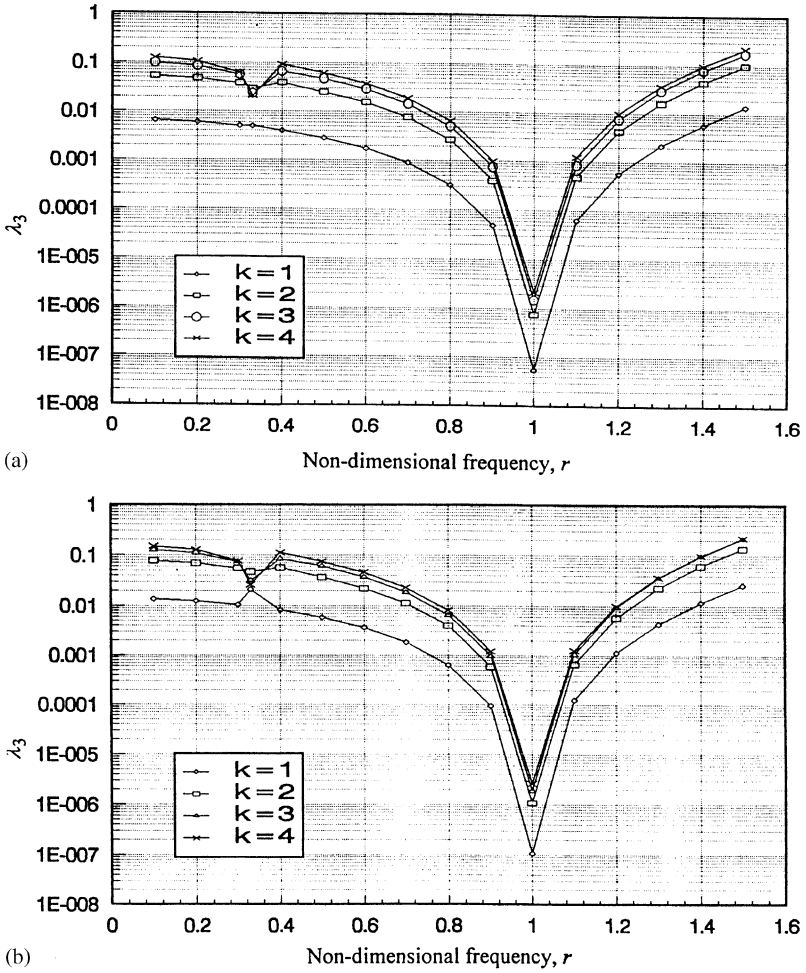

Fig. 3. Variation in excitation level for constant error: (a) error limit = 0.005, (b) error limit = 0.01.

frequency range for constant approximation errors (0.005 and 0.01) in the first response harmonic series. Obtaining such a plot during a practical application for parameter estimation is difficult for it requires a priori knowledge of the non-linear parameter itself. However, the excitation amplitude can be varied over the frequency range such that the first harmonic response amplitude is maintained constant. Fig. 4(a) typically shows such a variation of excitation amplitude for obtaining constant response harmonic amplitude. The consequent response is given in Fig. 4(b). Fig. 4(c) shows the consequent error for a different number of series terms. It can be observed that while the error is relatively higher near the natural frequency (10% error with $k = 3$), it is significantly less in comparison to what would have resulted for the constant excitation level case of Fig. 1. It can therefore be suggested that for estimation of first order FRF through Eq. (14), the

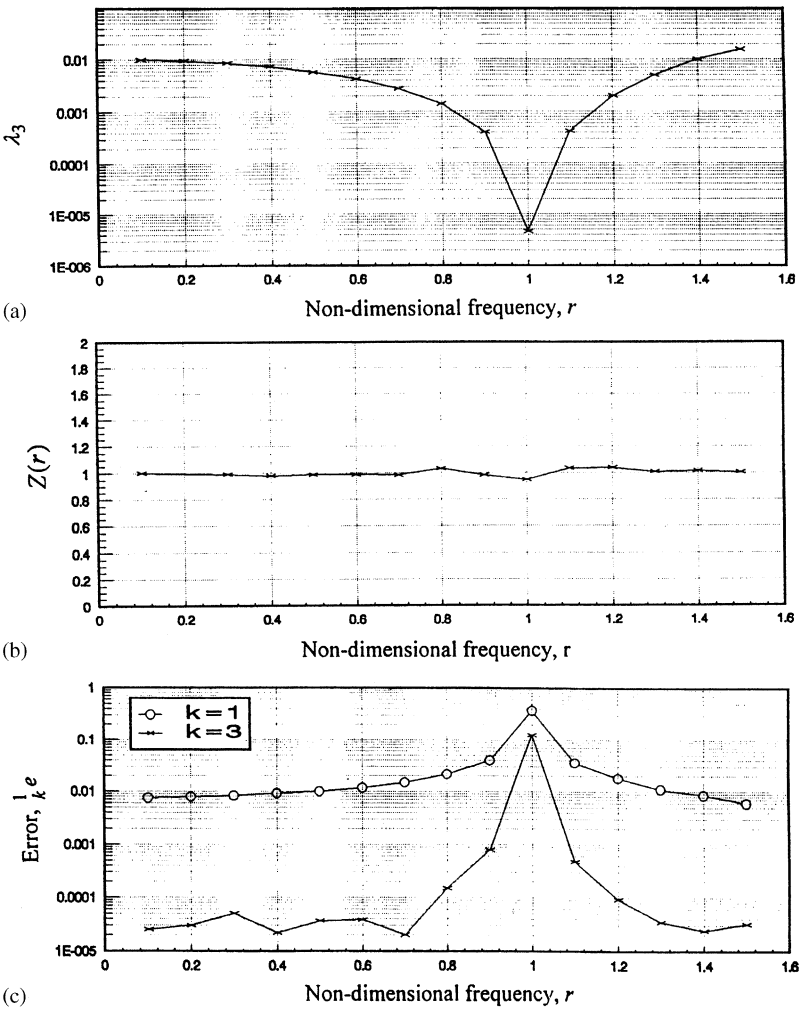

Fig. 4. (a) Excitation level for constant response harmonic amplitude, $Z(r)$, (b) response harmonic amplitude, $Z(r)$, (c) series approximation error for excitation level with constant $Z(r)$.

excitation level should be controlled in such a manner that the first harmonic level remains constant over the frequency range.

5. Measurability of higher order response harmonics

Higher order response harmonics for weakly non-linear systems are of much lower amplitude compared to the fundamental harmonic and may be of the same order as background vibration or measurement noise. This is illustrated in Fig. 5(a), where the non-dimensional third order response harmonic amplitude $Z(\omega_1+\omega_2+\omega_3)$ is plotted for a range of ω_1 and ω_2, while maintaining a constant $\omega_3/\omega_n = 0.2$. It can be seen that the third order harmonic $Z(\omega_1+\omega_2+\omega_3)$ is distinct along line $\boldsymbol{A}$ representing the frequency combinations $\omega_1+\omega_2+\omega_3=\omega_n$. On other regions of the frequency floor, the response strength is significantly small. Better signal/noise ratio would therefore be achieved for the third order harmonic if measurements are carried out along line $\boldsymbol{A}$, indicated in Fig. 5(a).

A single-term approximation of the non-dimensional response harmonic $Z(\omega_1+\omega_2+\omega_3)$ given by

$$Z(\omega_1+\omega_2+\omega_3)\approx\tfrac{3}{2}H_3(\omega_1/\omega_n,\omega_2/\omega_n,\omega_3/\omega_n) \tag{23}$$

is plotted in Fig. 5(b) over the frequency range. Fig. 5(c) gives the error between the 'exact' response and the single term approximation. It can be seen from Figs. 5(a) and (c), that the estimation error can be kept low, while maintaining high signal/noise ratio if measurements are made along line $\boldsymbol{A}$ representing the frequency combinations $\omega_1+\omega_2+\omega_3=\omega_n$. In case of single-tone excitation, it is obvious from the above that third order response harmonic, $X(3\omega)$, should be measured at or close to $3\omega=\omega_n$, i.e., $\omega=\omega_n/3$. The measurability of the third response harmonic in the case of a Duffing oscillator under single tone excitation is shown in Figs. 6(a) and (b). This has been done by defining a parameter as Measurability Index, $MI(m\omega)$, which is the ratio of mth response harmonic amplitude to the first harmonic amplitude, i.e.,

$$MI(m\omega)=X(m\omega)/X(\omega). \tag{24}$$

Measurability is maximum at one-third of the natural frequency and this maximum value can be termed as peak measurability factor. Figs. 6(a) and (b) also show the dependence of peak measurability factor on excitation amplitude and damping. It can be seen from Fig. 2(b) that the series approximation error in third harmonic for $\lambda_3=0.01$ (which gives 10% measurability) can be restricted within 1.5% with four series terms. Based on the above observations, it is suggested that the third harmonic should be measured around a set of frequencies very close to one-third of the natural frequency and on both sides of it. The excitation level should be kept constant for this close frequency band and can be set to obtain a desired peak measurability value (up to 10%).

6. Detection of the sign of non-linear parameter

The non-linear parameter k_3 is obtained through the linear regression of Eq. (15). The regression is done with the magnitude of the complex quantities and hence the estimated values represent only the magnitude of the non-linear parameters and not their sign. Sign of the

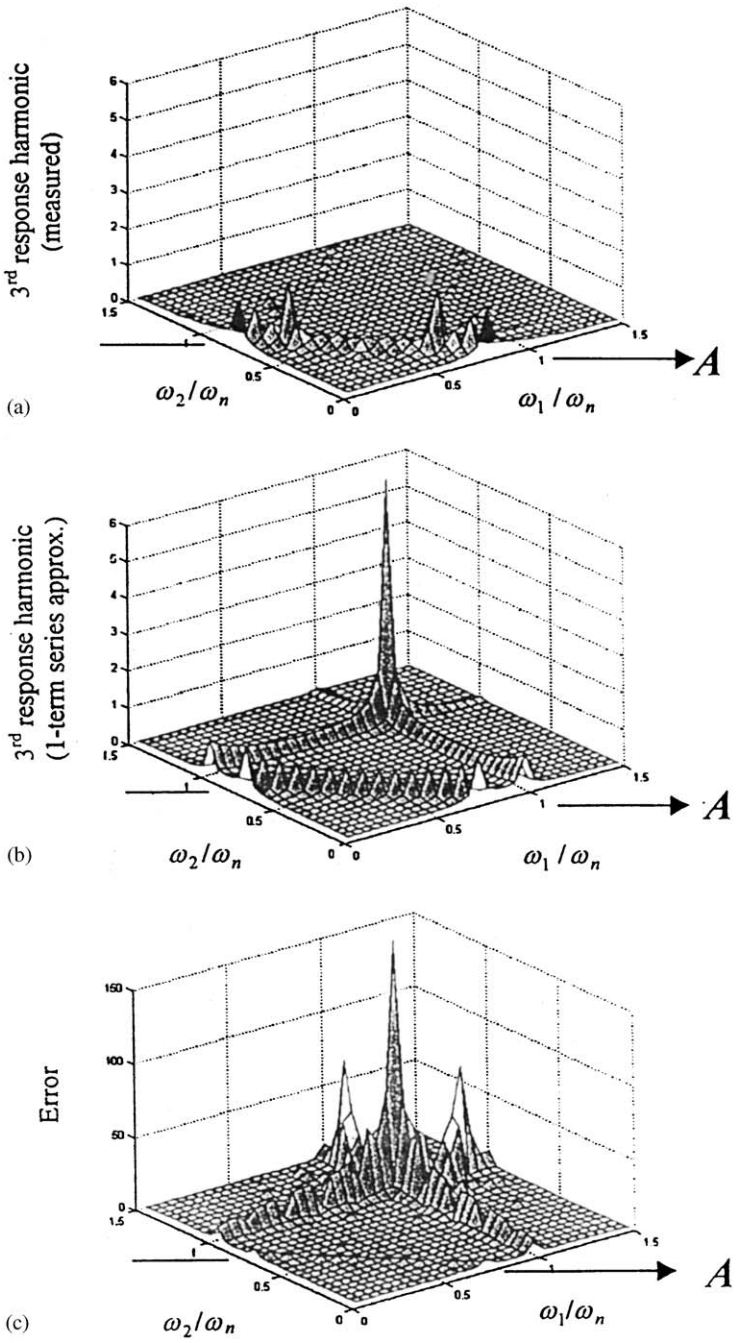

Fig. 5. Third harmonic amplitude, $Z(\omega_1+\omega_2+\omega_3)$ and error in single-term series approximation [$\omega_3/\omega_n = 0.2$; $\lambda_3 = 0.01$]: (a) exact response harmonic amplitude, (b) single-term series approximation, (c) error in single-term series approximation.

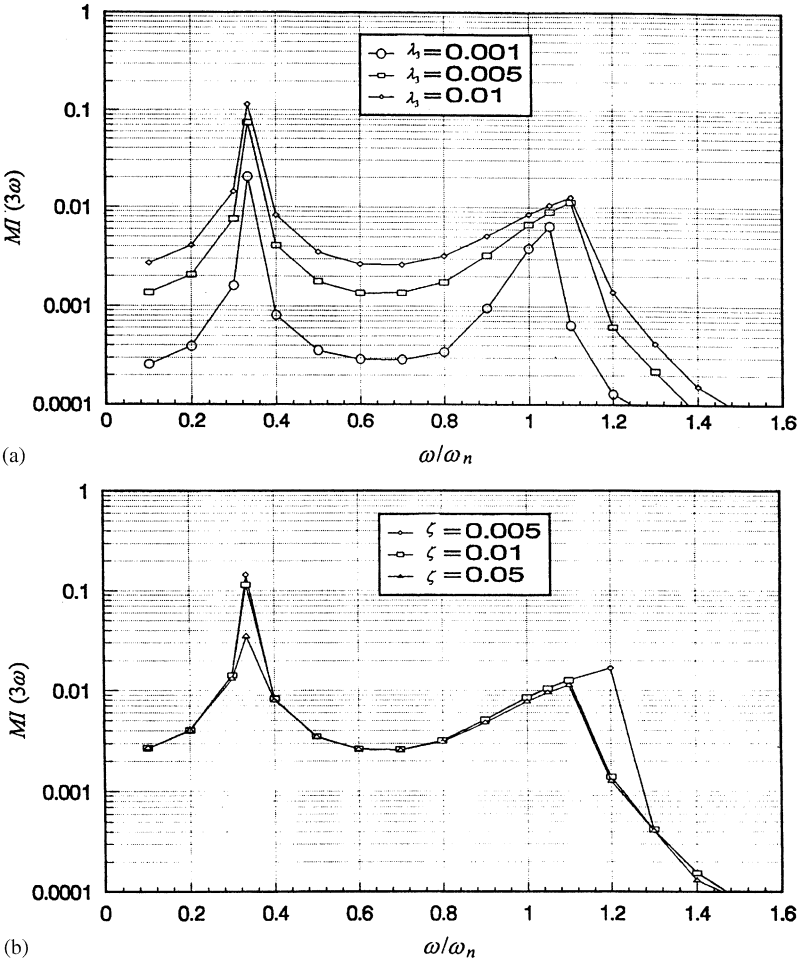

Fig. 6. Measurability index, $MI(3\omega)$: (a) for different excitation levels with $\zeta = 0.01$, (b) for different damping with $\lambda_3 = 0.01$.

non-linear parameter, k_3, can be detected through observations of change of sign of the real part of measured third harmonic amplitudes during transition of excitation frequency across one-third of the natural frequency. Rewriting Eq. (16) for synthesis of the kernel factor

$$\Gamma_3(3\omega) = -H_1^3(\omega)H_1(3\omega),$$

one can note that for $\omega < \omega_n/3$, both $H_1(\omega)$ and $H_1(3\omega)$ have positive real parts, which means that the kernel factor $\Gamma_3(3\omega)$ will have a negative real part. Consequently, the third order kernel transform $H_3(\omega, \omega, \omega)$, in Eq. (15), will also have a negative real part for positive k_3. For $\omega_n > \omega > \omega_n/3$, $H_1(\omega)$ will have a positive real part while the real part of $H_1(3\omega)$ will bear negative sign. The kernel factor, $\Gamma_3(3\omega)$, and $H_3(\omega, \omega, \omega)$ will have a positive real part for positive value of the non-linear parameter k_3.

7. Numerical illustration

The parameter estimation procedure is numerically illustrated for a Duffing oscillator

$$m\ddot{x}(t) + c\dot{x}(t) + k_1 x(t) + k_3 x^3(t) = f(t), \tag{25}$$

with the following parameters:

$$k_1 = 1.0 \times 10^7\ \mathrm{N/m}, \quad m = 1.0\ \mathrm{kg}, \quad c = 64.3\ \mathrm{Ns/m}, \quad k_3 = 1.0 \times 10^{19}\ \mathrm{N/m^3}.$$

The above stiffness parameters are selected to correspond to a typical rotor bearing system with rolling element bearings [11], and the damping coefficient is selected to correspond 1% damping ratio (i.e., $\zeta = 0.01$).

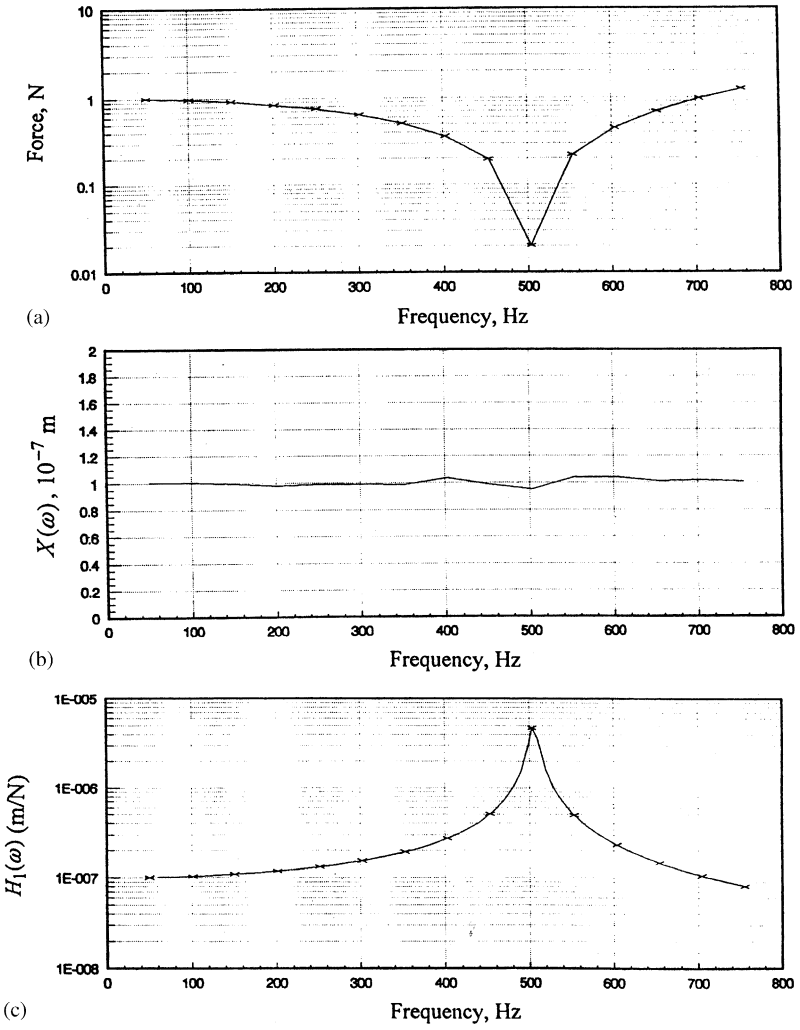

Fig. 7. (a) Variation in excitation levels for constant response harmonic amplitude $X(\omega) = 1.0 \times 10^{-7}$ m, (b) measured response harmonic amplitude, $X(\omega)$, (c) preliminary estimates of first order kernel transform, $H_1(\omega)$.

7.1. Preliminary linear estimates

Numerical solution, $x(t)$, to the equation of motion (25) is obtained through fourth order Runge–Kutta integration algorithm. Response harmonics $X(\omega)$ and $X(3\omega)$ are separated by harmonic filtering. The first response harmonic, $X(\omega)$, is measured with excitation level adjusted so as to give a constant response amplitude of 1.0×10^{-7} m. A wide range of excitation frequency is considered from 50 to 750 Hz, covering the natural frequency $\omega_n = 503$ Hz. Fig. 7(a) shows the excitation amplitude employed at various frequencies to obtain the constant harmonic amplitude $X(\omega)$ shown in Fig. 7(b). Preliminary estimate of the first order kernel $H_1(\omega)$ from $X(\omega)$ using Eq. (12a) is plotted in Fig. 7(c). Linear parameters are estimated through curve fitting over the estimated $H_1(\omega)$ values. The preliminary estimates are $k_1 = 1.0074 \times 10^7$ N/m, $m = 0.9999$ kg, $\varsigma = 0.01055$.

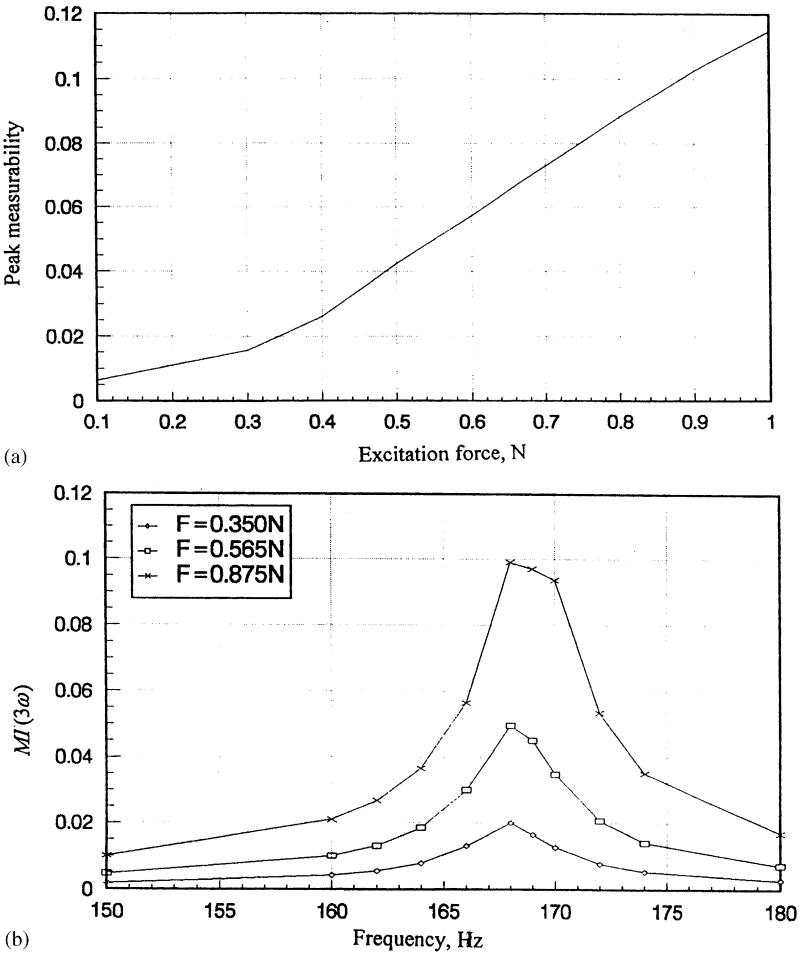

Fig. 8. (a) Peak measurability factor at different excitation levels, (b) variation in measurability index, $MI(3\omega)$ around $\omega_n/3$.

7.2. Non-linear estimates

For estimation of non-linear parameters, the plot of third harmonic peak measurability factor is obtained for various excitation amplitudes (Fig. 8(a)). Peak measurability factors are typically chosen as 2%, 5% and 10% and the excitation force amplitudes required for these measurabilities of the third harmonic are read from Fig. 8(a) to be 0.35, 0.565 and 0.875 N, respectively. The recursive iteration method is illustrated for the three cases of measurability chosen above. Four excitation frequencies (164.0, 166.0, 170.0 and 172.0 Hz) are selected close to one-third of the natural frequency ($\omega_n/3 = 167.7$ Hz) for the measurement of third response harmonic. Fig. 8(b) shows the measurability variation in the neighborhood of this band of frequencies.

Case (i) (2% *peak measurability*; *force amplitude* = 0.35 N): Harmonic excitation of amplitude 0.35 N is applied at the four selected frequencies and third response harmonic amplitude $X(3\omega)$ filtered from the response is shown in Figs. 9(a)–(d). Preliminary estimation in accordance with Eqs. (15) and (16), gives the value of the non-linear parameter, $k_3 = 1.0332 \times 10^{19}$ N/m^3. This estimate is in error by 3.32%. With subsequent iterations, this estimate converges to a value $k_3 = 1.0053 \times 10^{19}$ N/m^3. The convergence pattern is displayed in Fig. 10(a). (Iteration is stopped when the change in successive estimates of k_3 becomes less than 0.1%.) Significant improvement

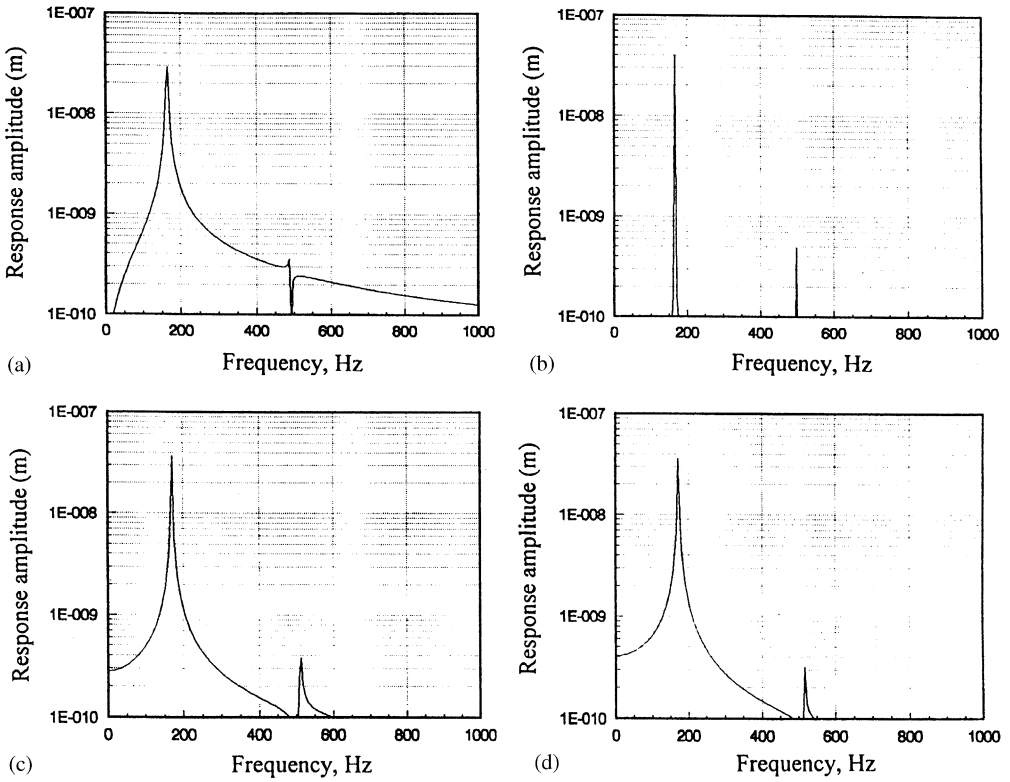

Fig. 9. Response spectra with force amplitude = 0.35 N [Case (i): 2% peak measurability]: (a) excitation at 164 Hz, (b) excitation at 166 Hz, (c) excitation at 170 Hz, (d) excitation at 172 Hz.

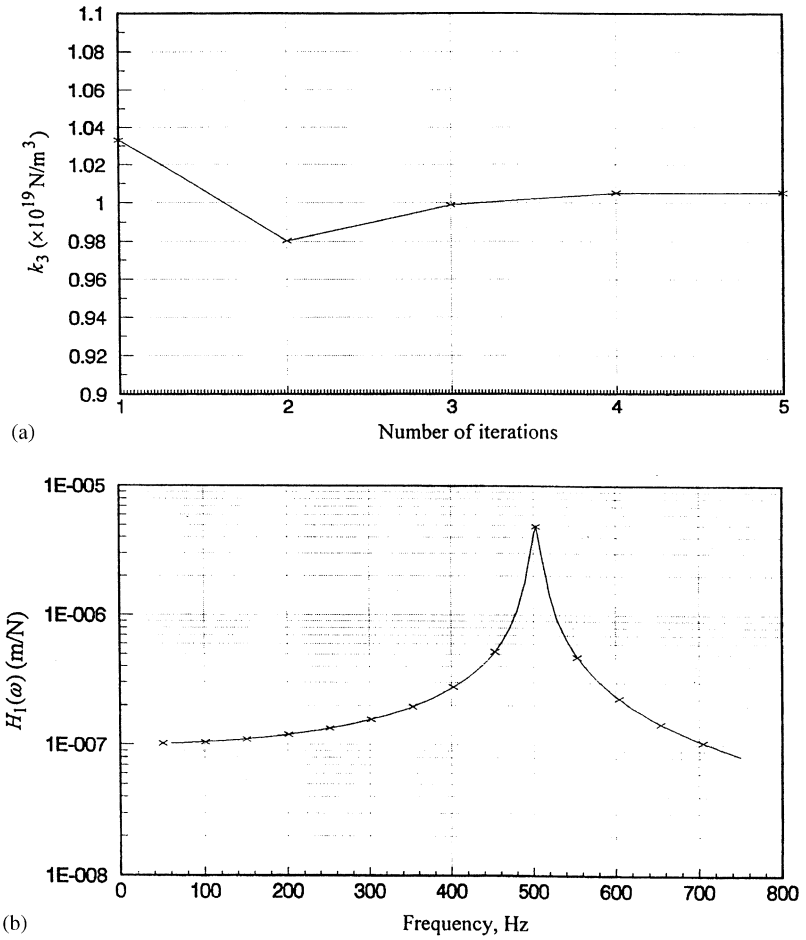

Fig. 10. (a) Iterative estimates of k_3 [Case (i): 2% peak measurability], (b) final estimate of first order kernel transform, $H_1(\omega)$ [Case (i): 2% peak measurability].

in the estimated value is achieved with iterations, whereby the error can be seen to come down from 3.32% to 0.53%. The final estimate of the first order kernel transform, $H_1(\omega)$, is shown in Fig. 10(b) and the estimated linear parameters are

$$k_1 = 0.9998 \times 10^7 \text{ N/m}, \quad m = 0.9999 \text{ kg}, \quad \varsigma = 0.01024.$$

Case (ii): (5% *peak measurability*; *force amplitude* = 0.565 N): Figs. 11(a)–(d) show the response spectrum at the four frequencies selected for measurements. The estimate for the non-linear parameter k_3, in this case, converges from a preliminary value of $1.0309 \times 10^{19}\text{N/m}^3$ to a final value of $1.0065 \times 10^{19}\text{ N/m}^3$, as shown in Fig. 12(a). The errors are 3.09% for the preliminary value and 0.65% for the final value. The final estimate of first order kernel transform, $H_1(\omega)$, is

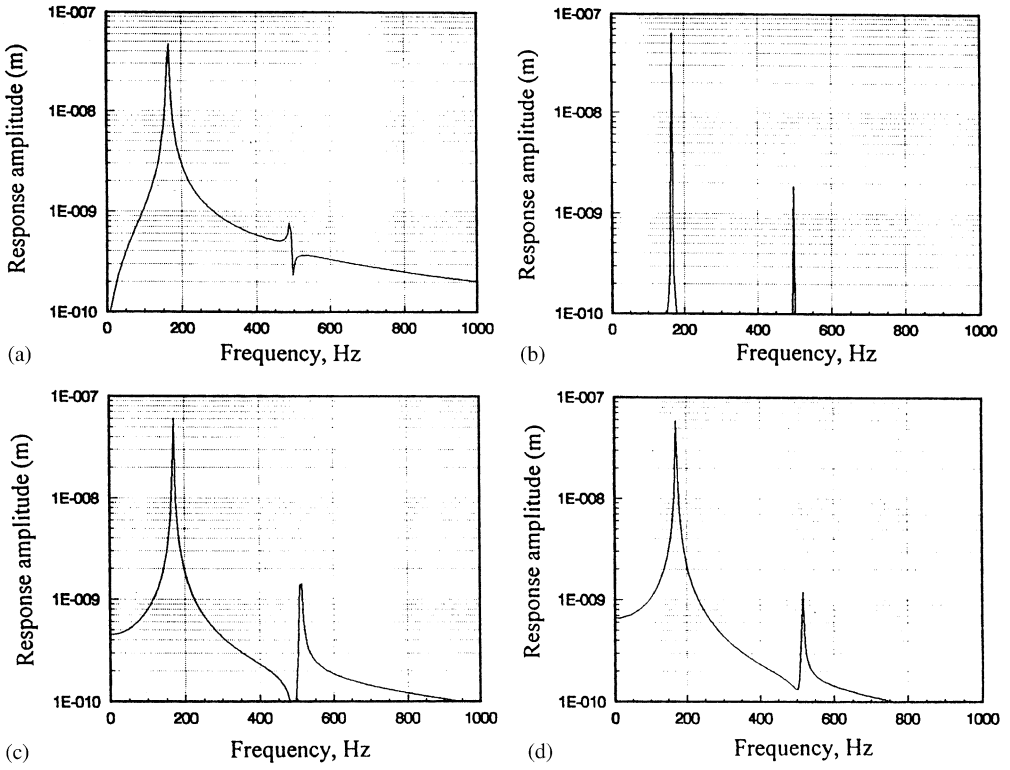

Fig. 11. Response spectra with force amplitude = 0.565 N [Case (ii): 5% peak measurability]: (a) excitation at 164 Hz, (b) excitation at 166 Hz, (c) excitation at 170 Hz, (d) excitation at 172 Hz.

shown in Fig. 12(b) and the estimated linear parameters are

$$k_1 = 0.9998 \times 10^7\ \mathrm{N/m},\ \ m = 0.9999\ \mathrm{kg},\ \ \varsigma = 0.01023.$$

Case (iii) (10% *peak measurability*; *force amplitude* = 0.875 N): Figs. 13(a)–(d) show the response spectrum at the four selected frequencies. Estimate of the non-linear parameter k_3 converges from an initial value of $1.0520 \times 10^{19}\ \mathrm{N/m^3}$ to a final value of $1.0146 \times 10^{19}\ \mathrm{N/m^3}$ as shown in Fig. 14(a). The estimation error is 5.2% for the preliminary value and 1.46% for the final value. The final estimation of first order kernel transform is shown in Fig. 14(b) and the estimated linear parameters are

$$k_1 = 0.9996 \times 10^7\ \mathrm{N/m},\ \ m = 0.9999\ \mathrm{kg},\ \ \varsigma = 0.01029.$$

The summary of the results in the three cases is given in Table 1.

It is evident that while significant improvement in estimates is achieved with iteration, the error is strongly linked to the excitation amplitude used in third harmonic measurement. A higher excitation level (force amplitude = 0.875 N), while providing a better measurability of 10% also gives a relatively high error of 1.46%. The excitation amplitude of 0.35 N gives relatively lesser error of 0.53%, but reduces the measurability of third harmonic to 2%. Estimates of mass and stiffness parameters do not show any significant trend with iterations. Damping estimates,

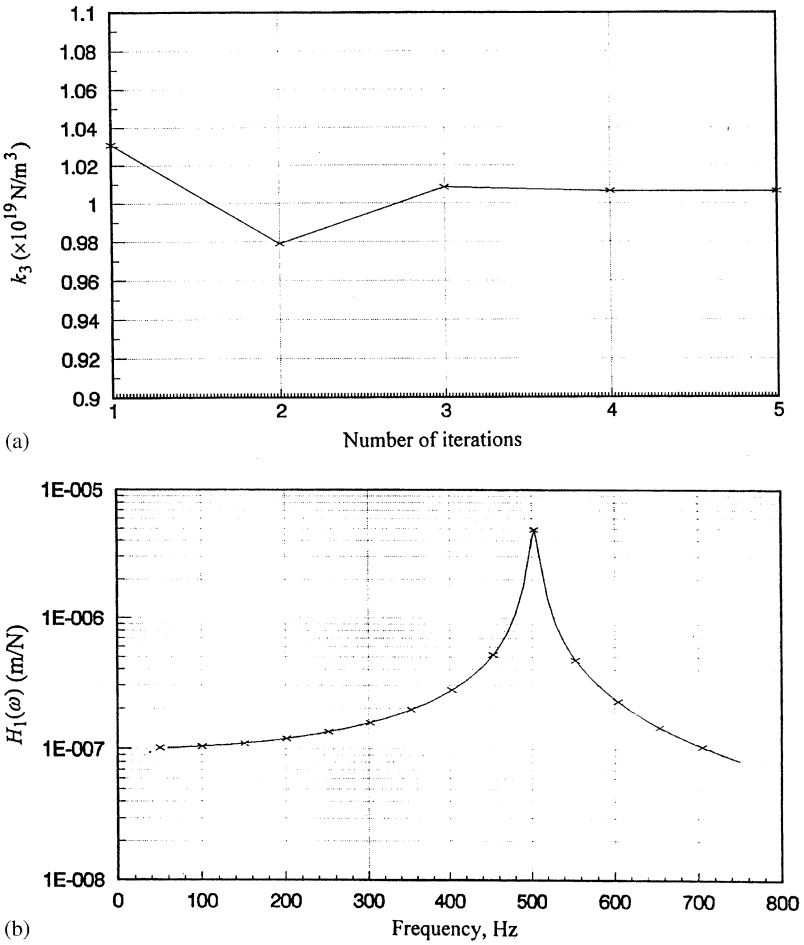

Fig. 12. (a) Iterative estimates of k_3 [Case (ii): 5% peak measurability], (b) final estimate of first order kernel transform, $H_1(\omega)$ [Case (ii): 5% peak measurability].

however, get refined with iteration. These improvements in damping estimates play a numerically critical role during the estimation of the non-linear parameter k_3.

7.3. *Influence of measurement noise*

To investigate the robustness of the iterative procedure against the external noise, white noise is generated and added to the response time history. Noise-to-signal ratio is typically selected as 5%. Fig. 15(a) shows a typical response time history for a response level of 1.0×10^{-7} m and Fig. 15(b) shows a randomly varying white noise with noise to signal ratio of 5%. The combined time history is shown in Fig. 15(c). The noisy response data are then processed for the estimation of the parameters. Linear parameters are found to be

$$k_1 = 0.9998 \times 10^7 \text{ N/m}, \quad m = 0.9999 \text{ kg}, \quad \varsigma = 0.01028.$$

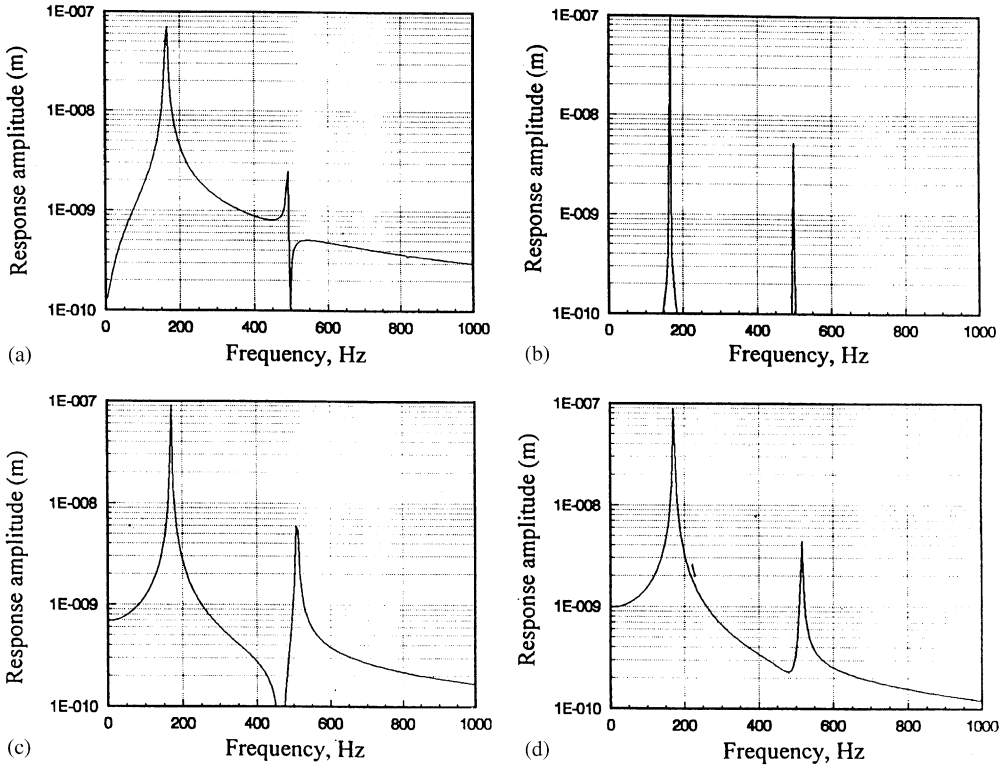

Fig. 13. Response spectra with force amplitude = 0.875 N [Case (iii): 10% peak measurability]: (a) excitation at 164 Hz, (b) excitation at 166 Hz, (c) excitation at 170 Hz, (d) excitation at 172 Hz.

Estimated values of the non-linear parameter k_3, in the presence of 5% noise, under different measurability conditions are shown in Table 2 along with the estimation values under zero noise condition obtained in Section 7.2. The results in Table 2 indicate the robustness of the estimation algorithm in the presence of measurement noise.

8. Conclusion

A new parameter estimation procedure based on recursive evaluation of Volterra kernels is presented here. The procedure is developed through a detailed convergence and error analysis of the finite term response series. Problems with measurability of higher order harmonic amplitudes have been investigated. A selection criterion is suggested for the excitation level and frequency band for optimum measurability of higher harmonics. The procedure yields good non-linear estimates, with suitably designed experiments, where excitation amplitudes and frequencies are chosen according to the discussed guidelines. The estimation algorithm is also tested and found robust against random measurement noise.

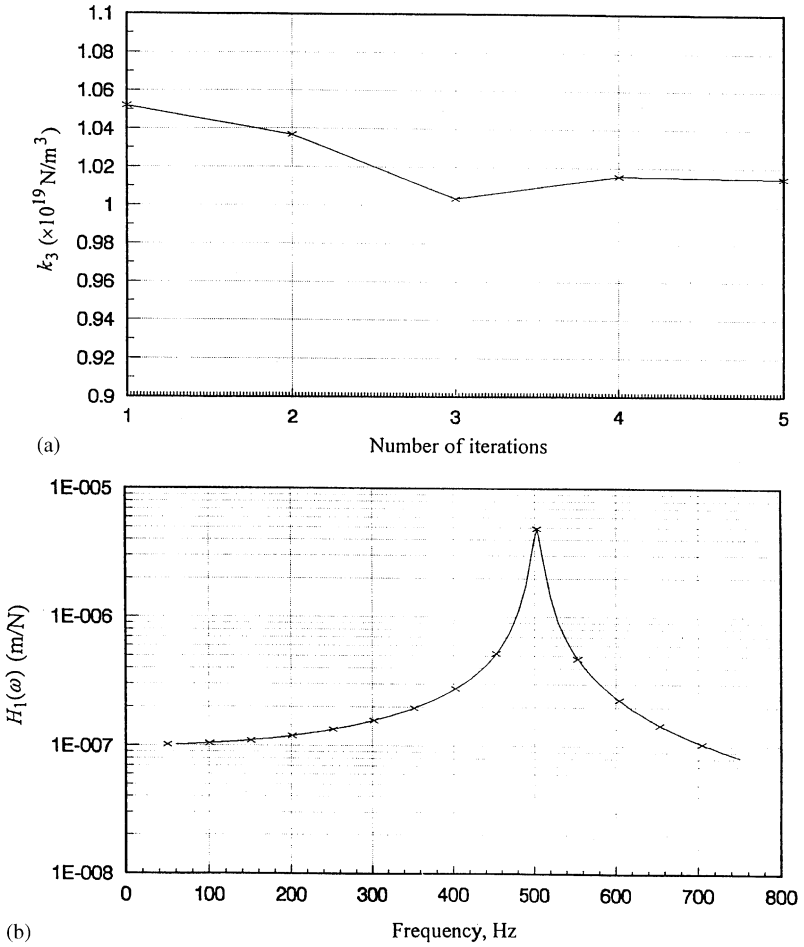

Fig. 14. (a) Iterative estimation of k_3 [Case (iii): 10% peak measurability], (b) final estimate of first order kernel transform, $H_1(\omega)$ [Case (iii): 10% peak measurability].

Table 1
Estimates under different measurability conditions

	$k_1 \times 10^7$ N/m		m (kg)		ξ		$k_3 \times 10^{19}$ N/m^3	
	Estimate	Error (%)	Estimate	Error (%)	Estimate	Error (%)	Estimate	Error (%)
Preliminary estimates	1.0074	0.74	0.9999	0.01	0.01055	5.5	1.0332	3.32
							1.0309	3.09
							1.0520	5.20
Final estimates Case (i)	0.9998	0.02	0.9999	0.01	0.01024	2.4	1.0053	0.53
Final estimates Case (ii)	0.9998	0.02	0.9999	0.01	0.01023	2.3	1.0065	0.65
Final estimates Case (iii)	0.9996	0.04	0.9999	0.01	0.01029	2.9	1.0146	1.46

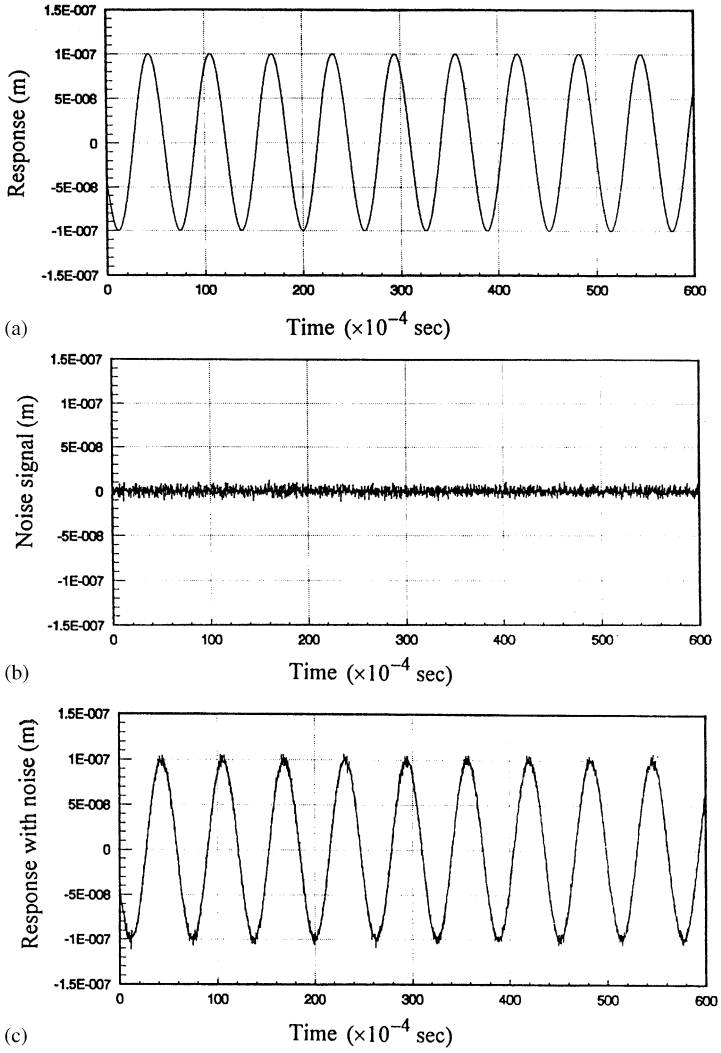

Fig. 15. Response measurement in presence of noise (noise to signal ratio 5%): (a) response without noise, (b) noise signal, (c) response with 5% noise.

Table 2
Effect of noise in parameter estimation

Measurability condition	k_3 ($\times 10^{19}$ N/m^3) with 5% noise	k_3 ($\times 10^{19}$ N/m^3) with zero noise
Case (i)	1.0069	1.0053
Case (ii)	1.0080	1.0065
Case (iii)	1.0150	1.0146

Acknowledgements

The authors wish to express their thanks to the financial aid being provided by the Propulsion Panel of Aeronautical Research and Development Board, Ministry of Defence, Government of India, in carrying out the study.

References

[1] S. Boyd, Y.S. Tang, L.O. Chua, Measuring Volterra kernels, IEEE Transactions on Circuits and Systems, CAS-30 (8) (1983) 571–577.
[2] L.O. Chua, Y. Liao, Measuring Volterra kernels (II), International Journal of Circuit Theory and Applications 17 (1989) 151–190.
[3] S.J. Gifford, G.R. Tomlinson, Recent advances in the application of functional series to nonlinear structures, Journal of Sound and Vibration 135 (2) (1989) 289–317.
[4] D.M. Storer, G.R. Tomlinson, Recent developments in the measurement and interpretation of higher order transfer functions from nonlinear structure, Mechanical Systems and Signal Processing 7 (2) (1993) 173–189.
[5] S.J. Gifford, Estimation of second and third order frequency response functions using truncated models, Mechanical Systems and Signal Processing 7 (2) (1993) 145–160.
[6] R. Haber, H. Unbehauen, Structure identification of nonlinear dynamic systems—a survey on input/output approaches, Automatica 26 (4) (1990) 651–677.
[7] G.R. Tomlinson, G. Manson, G.M. Lee, A simple criterion for establishing an upper limit to the harmonic excitation level of the Duffing oscillator using the Volterra series, Journal of Sound and Vibration 190 (5) (1996) 751–762.
[8] A. Chatterjee, N.S. Vyas, Convergence analysis of Volterra series response of nonlinear systems subjected to harmonic excitation, Journal of Sound and Vibration 236 (2) (2000) 339–358.
[9] G.M. Lee, Estimation of nonlinear system parameters using higher order frequency response functions, Mechanical Systems and Signal Processing 11 (2) (1997) 219–228.
[10] D.J. Ewins, Modal Testing: Theory and Practice, Research Studies Press, Baldock, 1984.
[11] A.A. Khan, N.S. Vyas, Application of Volterra and Wiener theories for nonlinear parameter estimation in a rotor-bearing system, Nonlinear Dynamics 24 (3) (2001) 285–304.